INTERNATIONAL JOURNAL FOR NUMERICAL METHODS IN FLUIDS
Int. J. Numer. Meth. Fluids **28**: 737–757 (1998)

ACCURACY AND PERFORMANCE OF NUMERICAL WALL BOUNDARY CONDITIONS FOR STEADY, 2D, INCOMPRESSIBLE STREAMFUNCTION VORTICITY

WILLIAM F. SPOTZ*

National Center for Atmospheric Research, PO Box 3000, Boulder, CO 80307-3000, USA

SUMMARY

Three recent papers have studied fourth-order compact discretizations of the streamfunction vorticity equations. They differed primarily in how the no-slip wall boundary conditions were handled. In this paper, these different formulas are compared to one another, as well as to three newly proposed formulas. Special consideration is paid to the truncation errors; in particular, it is shown that many well-known formulations are actually more accurate by $O(h)$ than previously reported, where h is the mesh size. These new theoretical error rates are confirmed with an analytical model problem. The different formulas are then compared with published driven cavity results, both in terms of accuracy and performance, and the newly proposed high-order Jensen formula is judged to have the marginally best combination of these properties. © 1998 John Wiley & Sons, Ltd.

KEY WORDS: high-order; compact; finite difference; no-slip; no-penetration; driven cavity

1. INTRODUCTION

Fourth-order-accurate, compact, finite difference approximations to the model convection diffusion equation have been proposed by Gupta, Manohar and Stephenson [1,2], Dennis and Wing [3], MacKinnon and Carey [4], Dennis and Hudson [5], and MacKinnon and Johnson [6]. Although these various discretizations are constructed via different mechanisms, the resulting stencil coefficients are equivalent [6], and represent a class of methods which will be referred to here as high-order compact (HOC) schemes.

Compact schemes use pointwise stencils which are restricted, by definition, to the set of points on the cells supported by that point. They are desirable because they do not require special formulations near boundaries and are efficient candidates for parallelization by domain decomposition. HOC schemes are attractive for these reasons, but also for their higher accuracy, and for the fact that they suppress numerical oscillations without the need for artificial viscosity [6,7].

The streamfunction vorticity (ψ, ζ) representation of the steady, 2D, incompressible Navier–Stokes equations is, by virtue of its form, an obvious candidate for the HOC scheme. In 1991, Gupta [8] applied his fourth-order compact formulation to the solution of these equations. This study was followed more recently by similar research by Li *et al.* [9], and Spotz and Carey [10].

* Correspondence to: National Center for Atmospheric Research, PO Box 3000, Boulder, CO 80307-3000, USA.

CCC 0271–2091/98/140737–21$17.50

Received March 1997
Revised September 1997

In light of the equivalency of the underlying numerical methods, it is not surprising that the three streamfunction vorticity studies produced very similar results. All three develop fourth-order compact approximations to the velocity components; all three solve the standard benchmark driven cavity problem in which a moving lid drives the fluid in a unit cavity; and all three obtain accurate solutions for up to at least $Re = 1000$ on relatively coarse meshes without a highly sophisticated non-linear iteration or continuation technique. Gupta solves up to $Re = 2000$ using point-successive overrelaxation (SOR) and successive approximations. Li *et al.* solve up to $Re = 7500$ using point-SOR, Newton's method, and continuation. Both studies make qualitative comparisons of streamfunction and vorticity contour plots to previously reported results in the literature for much finer meshes. Spotz and Carey solve up to $Re = 1000$ using the generalized minimal residual (GMRES) method and successive approximation, and also include cross-sectional comparisons of velocity and vorticity to illustrate the higher accuracy.

The primary difference in the discretizations among the three papers is the treatment of the no-slip wall boundary condition, and this topic is explored in the present study. The HOC interior formulation has motivated a search for HOC boundary conditions, but a robust formulation has remained elusive. In fact, the attempt to find any appropriate numerical treatment for the no-slip wall boundary condition for the (ψ, ζ) equations is a long and somewhat controversial one (see, e.g. References [11–13]), and is more difficult in the context of a high-order scheme if maintenance of the accuracy on a compact stencil is required.

There seem to be two issues of concern [9]. First, the no-slip and no-penetration velocities are easily related to the streamfunction, but not so easily related to the vorticity on the boundary. In fact, Gresho [13] emphatically insists that 'there are no BCs for the vorticity', and that none are needed. Second, it has not been clear whether less accuracy on the boundary would degrade or pollute the global accuracy. Certainly, one would expect to see a degradation in accuracy for this case (at least for a problem solved on a constant sized mesh, as they are here), yet experimental evidence has contradicted logic [14].

Surprisingly, these two concerns about the physics and accuracy are much more tightly connected than they might appear at first glance, and can both be addressed with a single re-interpretation. Use of the HOC scheme originally facilitated this new interpretation, and should clear up some longstanding and common misconceptions.

In the following section, the various wall boundary condition formulas to be studied are derived and a rigorous analysis of truncation error is made. The order of accuracy and relative pollution due to various boundary condition treatments are determined experimentally in Section 3. The performance of these formulas is compared in Section 4, to determine which gives the most accuracy with the least amount of computational 'work.' Finally, in Section 5, these boundary condition formulas are compared with respect to their corresponding driven cavity results.

2. WALL BOUNDARY CONDITION FORMULATIONS

The steady, 2D, incompressible, streamfunction vorticity equations can be summarized on a simply-connected domain, Ω with no-slip, no-penetration boundary conditions on $\partial\Omega$, as

$$u = \frac{\partial \psi}{\partial y} \quad \text{on } \Omega, \tag{1}$$

$$v = -\frac{\partial \psi}{\partial x} \quad \text{on } \Omega, \tag{2}$$

$$-\nabla^2 \psi = \zeta \quad \text{on } \Omega, \tag{3}$$

$$-\nabla^2 \zeta + Re\boldsymbol{V} \cdot \nabla \zeta = f \quad \text{on } \Omega, \tag{4}$$

$$\frac{\partial \psi}{\partial s} = 0 \quad \text{on } \partial\Omega, \tag{5}$$

$$\frac{\partial \psi}{\partial n} = \pm V_w \quad \text{on } \partial\Omega, \tag{6}$$

where $\boldsymbol{V} = (u, v)$ is the velocity vector, Re is the Reynolds number, f is a prescribed forcing function, n is the local direction normal to $\partial\Omega$, s is the local direction tangent to $\partial\Omega$, and V_w is the tangential wall velocity. Equations (1)–(6) are a complete specification of the problem to be solved. Note that the two boundary conditions, Equations (5) and (6), do not involve the vorticity. Thus, if we attempt to solve Equation (4) alone (e.g. as part of a block-iterative algorithm applied to the fully coupled system), the system will be underspecified because there is no immediate way to obtain vorticity values on $\partial\Omega$.

The reader is referred to References [8–10] for fourth-order, compact discretizations of Equations (1)–(4), although only Reference [10] includes the effects of f in Equation (4) and Reference [9] eliminates u and v from the system. Equation (5) is easily satisfied by requiring $\psi(\partial\Omega)$ to be a constant (usually zero by convention). The discretization of Equation (6) is the focus of the following sections.

2.1. Jensen's formulation

Gupta chose to use Jensen's formulation (so named by Roache [15], also known as Briley's formula) which can be derived as follows. Let subscript j represent the grid point located a distance jh from any boundary. Using Taylor series, we can write

$$\psi_1 + a\psi_2 = (1+a)\psi_0 + (1+2a)h\left.\frac{\partial \psi}{\partial n}\right|_0 + (1+4a)\frac{h^2}{2}\left.\frac{\partial^2 \psi}{\partial n^2}\right|_0 + (1+8a)\frac{h^3}{6}\left.\frac{\partial^3 \psi}{\partial n^3}\right|_0 + O(h^4), \tag{7}$$

for an arbitrary constant a. We can substitute Equations (6) and (3) into (7), utilizing the fact that $\partial^2\psi/\partial s^2 = 0$ on a wall, and choose $a = -1/8$ to cancel the h^3 term, to yield

$$\psi_1 - \frac{1}{8}\psi_2 = \frac{7}{8}\psi_0 \pm \frac{3h}{4}V_w - \frac{h^2}{4}\zeta_0 + O(h^4).$$

We can further scale by $4/h^2$ and rearrange to get Jensen's formula,

$$\zeta_0 = \frac{7\psi_0 - 8\psi_1 + \psi_2}{2h^2} \pm \frac{3V_w}{h} + O(h^2). \tag{8}$$

For the driven cavity problem, $V_w = 0$ except on the moving lid, where $+V_w = u_0 = 1$. Technically, Equation (8) is non-compact, although in a decoupled algorithm, the non-compact part of the stencil is computed explicitly on the right-hand-side, and so has little effect on the matrix solution.

It is claimed [8,15–18] that Equation (8) is an $O(h^2)$ approximation of the vorticity on the boundary, by virtue of the second-order term which is dropped. However, the ultimate solution error is proportional to the *truncation error* (provided h is small enough), and the

truncation error is formally defined as the difference between the differential equation and its numerical approximation. Clearly, if we take the $\lim_{h\to 0}$, the term $3V_w/h$ in Equation (8) is unbounded. However, if Equation (8) is written instead as

$$\frac{h}{3}\zeta_0 = \frac{7\psi_0 - 8\psi_1 + \psi_2}{6h} \pm V_w + O(h^3), \tag{9}$$

and $\lim_{h\to 0}$ is used, the relation $\partial\psi/\partial n = \pm V_w$ is recovered. Therefore, the difference between Equation (6) and its approximation is the $O(h^3)$ term in Equation (9), not the $O(h^2)$ term in Equation (8). Numerical experiments in Section 3 will confirm this interpretation. This also forces us to interpret Equation (9) [or equivalently (8)], not as a Dirichlet-type boundary condition on the vorticity, but rather as a streamfunction/velocity boundary condition, in which the vorticity conveniently enters to model higher-order terms. This new interpretation should also help address the concern that there are no physical BCs for the vorticity, because the limiting case of Equation (9) makes no such claim.

2.2. The computational boundary method

Li *et al.* chose to handle the boundary conditions with what Huang and Yang [19] call the computational boundary method (CBM) and what Gresho [13] classifies as a 'modern' formulation. Using the same subscripting convention as for the Jensen formulation, use the fact that

$$\pm V_w = \left.\frac{\partial\psi}{\partial n}\right|_0 = \frac{-11\psi_0 + 18\psi_1 - 9\psi_2 + 2\psi_3}{6h} + O(h^3), \tag{10}$$

to set $\psi_1 = 11\psi_0/18 + \psi_2/2 - \psi_3/9 \pm V_w h/3$, where $V_w = 0$ for a stationary wall and 1 for a moving wall. The vorticity ζ_1 (i.e. the vorticity at distance h from the boundary) is determined by central differencing (3) as

$$\zeta_1 = -(\delta_x^2 + \delta_y^2)\psi_1 + O(h^2), \tag{11}$$

where δ_x^2 and δ_y^2 are the standard central difference operators for the second derivative in the x- and y-directions, respectively. Thus ζ_0 is never computed in the CBM and Equations (3) and (4) are solved with high-order compact formulas only on the interior, e.g. $[2h, 1-2h] \times [2h, 1-2h]$ when Ω is the unit square.

The logic behind this boundary condition is that no physical boundary condition is prescribed for ζ, therefore, no numerical boundary condition should be imposed on ζ. Furthermore, two boundary conditions are prescribed for ψ and therefore two numerical boundary conditions should be imposed on ψ. However, since vorticity is physically produced on the walls, the inability to compute ζ on the boundary is a liability. This also causes a problem when computing the velocities[1]. The HOC formulas (see Reference[10]) for u and v are

$$u_{ij} = \delta_y\psi_{ij} + \frac{h^2}{6}(\delta_y\zeta_{ij} + \delta_x^2\delta_y\psi_{ij}) + O(h^4),$$

$$v_{ij} = -\delta_x\psi_{ij} - \frac{h^2}{6}(\delta_x\zeta_{ij} + \delta_x\delta_y^2\psi_{ij}) + O(h^4),$$

where subscript ij now refers to point (x_i, y_j) on a uniform grid and δ_x and δ_y by are the standard central difference operators for the first derivatives in the x- and y-directions,

[1] Li *et al.* did not compute the velocities in Reference [9], and so avoided the problem.

respectively. Clearly, the fourth-order approximations to u_{ij} and v_{ij} require knowledge of ζ away from ij and thus the velocities at distance h from the wall will lose accuracy when ζ on the wall is undefined. Fortunately, this is only a local effect.

The use of Equation (10) violates Li's claim of 'genuine compactness', because it formally requires a four-point difference stencil in a single direction to model Equation (6). More importantly, the $O(h^2)$ and $O(h^3)$ truncation errors respectively introduced by Equations (11) and (10) are expected to pollute the $O(h^4)$ interior formulation, destroying much of the hard-won accuracy. Li *et al.* justify this choice by citing Hou and Wetton [14], who claim that a 'first-order vorticity boundary condition' will not degrade a second-order interior scheme. In reality, however, the boundary scheme used by Hou and Wetton is second-order (for the exact same reason that the Jensen formula is third-order—see the previous and following sections), so their failure to observe pollution is not surprising.

2.3. Second-order compact formulation

Spotz and Carey chose a third method of approximating the boundary conditions which mirrors their development of the interior discretization. Their interior HOC scheme was obtained by using the methodology developed by MacKinnon and Carey [4], MacKinnon and Johnson [6] and extended by Spotz [7]. This methodology can be summarized as follows: (1) given a governing elliptic differential equation, apply standard central differences, keeping the $O(h^2)$ truncation error terms in the formulation; (2) differentiate the governing equation to obtain expressions for the third and fourth derivatives in terms of lower-order and cross derivatives with compact, $O(h^2)$ central difference approximations; (3) substitute these approximate expressions back into the formulation, yielding an overall $O(h^4)$ scheme. This methodology can also be followed for approximating the no-slip boundary condition, with the exception that one-sided differencing must be used at the boundary, yielding additional $O(h)$ and $O(h^3)$ truncation error terms. Fortunately, there is more than just one governing equation available for making the required substitutions. The details of the derivation are less trivial than for the interior, but the end result is a set of compact higher-order difference expressions for the no-slip boundary condition. The boundary vorticity enters this expression naturally as a result of the HOC substitutions.

We now review and expand upon the high-order compact approximation to Equation (6) in Reference [10]. For definiteness, consider the top wall of a rectangular cavity. On an $M \times N$ discretization of mesh size h, we continue with the subscripting convention that ij refers to point (x_i, y_j), and thus have $+V_w = u_{iN} = 1$ for the driven cavity problem. By Taylor series,

$$u_{iN} = \left.\frac{\partial \psi}{\partial y}\right|_{iN} = \delta_y^- \psi_{iN} + \frac{h}{2}\left.\frac{\partial^2 \psi}{\partial y^2}\right|_{iN} - \frac{h^2}{6}\left.\frac{\partial^3 \psi}{\partial y^3}\right|_{iN} + \frac{h^3}{24}\left.\frac{\partial^4 \psi}{\partial y^4}\right|_{iN} + O(h^4), \tag{12}$$

where δ_y^- represents the one-sided backward difference operator in the y-direction. Using Equation (3), $\partial^2\psi/\partial y^2$ in Equation (12) can be written as

$$\left.\frac{\partial^2 \psi}{\partial y^2}\right|_{iN} = -\zeta_{iN} - \left.\frac{\partial^2 \psi}{\partial x^2}\right|_{iN}, \tag{13}$$

$$= -\zeta_{iN}, \tag{14}$$

using the fact that $\partial^2\psi/\partial x^2 = 0$ on a horizontal wall. A second-order compact (2OC) approximation can be easily obtained by substituting Equation (14) into (12) and neglecting the $O(h^2)$ and higher terms, i.e.

$$u_{iN} = \delta_y^- \psi_{iN} - \frac{h}{2}\zeta_{iN} + O(h^2), \tag{15}$$

where $u_{iN} = 1$. This is formally an $O(h^2)$ approximation to Equation (6), just as Equation (9) is an $O(h^3)$ approximation. Equation (15) is often scaled by $2/h$ in the literature, and rearranged to isolate ζ. It is written as

$$\zeta_{iN} = \frac{2}{h}(\delta_y^- \psi_{iN} - u_{iN}) + O(h), \tag{16}$$

which is an old and well-known formula (introduced as early as 1928 by Thom [20]) and incorrectly assumed to be an $O(h)$ Dirichlet-type boundary condition, when it is, in fact, more accurate than that.

2.4. Third-order compact formulation

Returning to our development of HOC boundary condition formulations, we can differentiate Equation (13) to get

$$\left.\frac{\partial^3 \psi}{\partial y^3}\right|_{iN} = -\left.\frac{\partial \zeta}{\partial y}\right|_{iN} - \left.\frac{\partial^3 \psi}{\partial x^2\,\partial y}\right|_{iN} = -\left.\frac{\partial \zeta}{\partial y}\right|_{iN} - \left.\frac{\partial^2 u}{\partial x^2}\right|_{iN} \tag{17}$$

$$= -\left.\frac{\partial \zeta}{\partial y}\right|_{iN}, \tag{18}$$

where Equation (1) is used to relate ψ and u and the fact that $\partial^2 u/\partial x^2$ is also zero on a horizontal wall. A third-order compact (3OC) approximation can be obtained by building upon the second-order boundary condition (15), substituting Equation (18) for the second-order truncation term in Equation (12), and utilizing a one-sided difference approximation for $\partial\zeta/\partial y$, so that

$$u_{iN} = \delta_y^- \psi_{iN} - \frac{h}{2}\zeta_{iN} + \frac{h^2}{6}\delta_y^- \zeta_{iN} + O(h^3). \tag{19}$$

Clearly, Equation (19) directly relates the vorticity on the boundary to interior vorticity data and must either be solved implicitly (along with the interior vorticity equations) or lagged to obtain values for ζ on the boundary.

Equation (19) was actually proposed in 1954 by Woods [21], but was originally thought to be an $O(h^2)$ boundary condition formula.

2.5. Fourth-order compact formulations

The present interior discretization is $O(h^4)$, therefore, an $O(h^4)$ boundary condition would be preferable to prevent a loss of accuracy. Continuing the development of Sections 2.3 and 2.4, Equation (17) can be differentiated to give

$$\left.\frac{\partial^4 \psi}{\partial y^4}\right|_{iN} = -\left.\frac{\partial^2 \zeta}{\partial y^2}\right|_{iN} - \left.\frac{\partial^3 u}{\partial x^2\,\partial y}\right|_{iN}. \tag{20}$$

Substituting Equation (20) into (12) shows that in order to obtain fourth-order accuracy, three approximations are needed at the wall: (1) an $O(h^2)$ approximation to $\partial\zeta/\partial y$; (2) an $O(h)$ approximation to $\partial^2\zeta/\partial y^2$; and (3) an $O(h)$ approximation to $\partial^3 u/\partial x^2 \partial y$. The third requirement is the easiest, simply

$$\left.\frac{\partial^3 u}{\partial x^2\,\partial y}\right|_{iN} = \delta_x^2 \delta_y^- u_{iN} + O(h). \tag{21}$$

Examining the terms involving $\partial\zeta/\partial y$ and $\partial^2\zeta/\partial y^2$,

$$-\frac{h^2}{6}\left.\frac{\partial\zeta}{\partial y}\right|_{iN} + \frac{h^3}{24}\left.\frac{\partial^2\zeta}{\partial y^2}\right|_{iN} = -\frac{h^2}{6}\left[\delta_y^-\zeta_{iN} + \frac{h}{2}\left.\frac{\partial^2\zeta}{\partial y^2}\right|_{iN} + O(h^2)\right] + \frac{h^3}{24}\left.\frac{\partial^2\zeta}{\partial y^2}\right|_{iN}$$
$$= -\frac{h^2}{6}\delta_y^-\zeta_{iN} - \frac{h^3}{24}\left.\frac{\partial^2\zeta}{\partial y^2}\right|_{iN} + O(h^4), \tag{22}$$

and using Equation (4),

$$\left.\frac{\partial^2\zeta}{\partial y^2}\right|_{iN} = Re\left(u_{iN}\left.\frac{\partial\zeta}{\partial x}\right|_{iN} + v_{iN}\left.\frac{\partial\zeta}{\partial y}\right|_{iN}\right) - \left.\frac{\partial^2\zeta}{\partial x^2}\right|_{iN} - f_{iN} = [Re\cdot u_{iN}\delta_x - \delta_x^2]\zeta_{iN} - f_{iN} + O(h^2), \tag{23}$$

where $v_{iN} = 0$ is used. Applying Equations (21)–(23) to the third-order terms in Equation (12), the complete, fourth-order compact (4OC) approximation to the boundary condition is

$$\delta_y^-\psi_{iN} - \left[\frac{h}{2} - \frac{h^2}{6}\delta_y^- - \frac{h^3}{24}(Re\cdot u_{iN}\delta_x - \delta_x^2)\right]\zeta_{iN} = u_{iN} + \frac{h^3}{24}(\delta_x^2\delta_y^- u_{iN} + f_{iN}) + O(h^4), \tag{24}$$

where the unknowns ψ and ζ are grouped on the left-hand-side. Similar conditions can be easily derived for the remaining three walls.

This formula was proposed by Spotz and Carey [10], and has been demonstrated to be satisfactory for stationary walls, but suffers from oscillations in the vorticity on the wall when $V_w \neq 0$ and the mesh size is too large relative to the Reynolds number. As a result, they resorted to Equation (19) for their driven cavity experiments. The oscillations are due to the term

$$\frac{h^3}{24}(Re\cdot u_{iN}\delta_x - \delta_x^2)\zeta_{iN}, \tag{25}$$

in Equation (24), which is proportional to the 1D central difference convection diffusion operator and is known to oscillate whenever the cell Peclet (or cell Reynolds) condition,

$$Re\cdot V_w\cdot h < 2,$$

is violated.

We hypothesize that using a non-oscillatory formula in place of Equation (25) should suppress the oscillations observed when using Equation (24). For example, the fourth-order compact formula with upwind correction (4OC/U) is

$$\delta_y^-\psi_{iN} - \left[\frac{h}{2} - \frac{h^2}{6}\delta_y^- - \frac{h^3}{24}(Re\cdot u_{iN}\delta_x^- - \delta_x^2)\right]\zeta_{iN} = u_{iN} + \frac{h^3}{24}(\delta_x^2\delta_y^- u_{iN} + f_{iN}) + O(h^4), \tag{26}$$

where δ_x^- would be replaced with δ_x^+ for the case where $u_{iN} < 0$.

It has also been proven [6] that the 1D HOC convection diffusion operator is non-oscillatory. The 4OC formula with HOC correction (4OC/H) is thus

$$\delta_y^-\psi_{iN} - \left[\frac{h}{2} - \frac{h^2}{6}\delta_y^- - \frac{h^3}{24}\left(Re\cdot u_{iN}\delta_x - \left(1 + \frac{Re^2 u_{iN}^2 h^2}{12}\right)\delta_x^2\right)\right]\zeta_{iN}$$
$$= u_{iN} + \frac{h^3}{24}(\delta_x^2\delta_y^- u_{iN} + f_{iN}) + O(h^4). \tag{27}$$

Note that the 1D HOC formula is derived by utilizing the 1D model equation. Thus its use in a 2D setting means that there are $O(h^2)$ terms which have been neglected, but since this formula is scaled by h^3, the overall $O(h^4)$ accuracy is maintained. The same is true for the $O(h)$ error introduced by the one-sided difference operator in the 4OC/U formula.

2.6. High-order Jensen formulation

The high-order compact ideas can be used to increase the accuracy of the Jensen formula from $O(h^3)$ to $O(h^4)$ while still maintaining a three-point stencil. Beginning with Equation (7), but including the $O(h^4)$ truncation error,

$$\psi_1 + a\psi_2 = (1+a)\psi_0 + (1+2a)h\left.\frac{\partial\psi}{\partial n}\right|_0 + (1+4a)\left.\frac{h^2}{2}\frac{\partial^2\psi}{\partial n^2}\right|_0 + (1+8a)\left.\frac{h^3}{6}\frac{\partial^3\psi}{\partial n^3}\right|_0 + (1+16a)\left.\frac{h^4}{24}\frac{\partial^4\psi}{\partial n^4}\right|_0 + O(h^5). \tag{28}$$

Setting $a = -1/16$ and using Equations (6) and (3) again to substitute for the first and second derivatives, as well as Equation (18) to substitute for the third derivative, gives

$$\frac{3h}{7}\zeta_0 + \left.\frac{2h^2}{21}\frac{\partial\zeta}{\partial n}\right|_0 + O(h^4) = \frac{1}{14h}(15\psi_0 - 16\psi_1 + \psi_2) \pm V_w,$$

where we have scaled the expression by $8/7h$ to get the proper truncation error. Thus, if we use

$$\left.\frac{\partial\zeta}{\partial n}\right|_0 = \frac{-3\zeta_0 + 4\zeta_1 - \zeta_2}{2h} + O(h^2),$$

to substitute for $\partial\zeta/\partial n$, the resulting high-order Jensen (HOJ) formula is

$$\frac{h}{21}(6\zeta_0 + 4\zeta_1 - \zeta_2) + O(h^4) = \frac{1}{14h}(15\psi_0 - 16\psi_1 + \psi_2) \pm V_w. \tag{29}$$

This expression is fourth-order-accurate, while using only three grid points for ψ and ζ.

3. ACCURACY STUDIES

The numerical schemes utilized here generate a class of linear systems which can be expressed in exact form as

$$\boldsymbol{A}\boldsymbol{u} = \boldsymbol{b} + \boldsymbol{\tau}, \tag{30}$$

where $\boldsymbol{A}$ is a coefficient matrix, $\boldsymbol{u}$ is a vector of nodal unknowns (representing either ψ or ζ or both), $\boldsymbol{b}$ is the right-hand-side vector, and $\boldsymbol{\tau} = \{\tau_i\}$ is the truncation error vector, where each component has the form

$$\tau_i = \sum_{p=m_i}^{\infty} C_{p,i} h^p.$$

Thus m_i represents the order of the leading truncation error term at a given grid point represented by index i, and would equal 4 for interior points, and either 2, 3, or 4 for boundary points, depending on the boundary formulation being used.

Of course, Equation (30) is not solved, but rather

$$\boldsymbol{A}\boldsymbol{u}_h = \boldsymbol{b},$$

where $\boldsymbol{u}_h$ is our approximate solution. The error is thus

$$\boldsymbol{e} = \boldsymbol{u} - \boldsymbol{u}_h = \boldsymbol{A}^{-1}\boldsymbol{\tau}. \tag{31}$$

It is easy to show that if $\boldsymbol{A}$ represents finite differencing on a mesh of constant h, then

$$e_i \propto h^m,$$

where $m = \min\{m_i\}$. In other words, a low-order approximation on the boundary will degrade a high-order interior approximation on a uniform mesh.

For the present numerical experiments, a global measure of the error is required. For an asymptotic local error of the form $e_i = O(h^m)$, the root mean square (RMS) error over N total grid points is also $O(h^m)$:

$$E \equiv \sqrt{\frac{\sum_i e_i^2}{N}} = \sqrt{\frac{N \times O(h^{2m})}{N}} = O(h^m).$$

This error norm can be used to determine convergence with respect to mesh size for the various boundary condition formulations, in order to verify the predicted convergence rates and to determine their relative accuracy. Therefore, an analytic model problem with known solution was chosen, so that the errors can be computed exactly. On domain $\Omega = [0, 1] \times [0, 1]$, let

$$\psi(x, y) = 8(x - x^2)^2(y - y^2)^2, \tag{32}$$

from which the exact velocities can be computed using Equations (1) and (2), and vorticity using Equation (3). The forcing function f which drives the problem, can then be obtained from Equation (4). This model problem is normalized such that $-1 \leq \zeta \leq 1$, and was chosen because $\psi = u = v = 0$ on $\partial\Omega$, and thus the no-slip, no-penetration wall boundary condition holds. Note that since the wall velocities are zero, the different permutations of the 4OC formulas collapse to the same discretization.

Experiments with the fourth-order, HOC interior discretizations were run at mesh sizes of $h = 1/4$, $1/8$, $1/16$, $1/32$ and $1/64$. Also, $Re = 0$ was used to further isolate the pollution of the boundary condition formulas. We observe the RMS of the vorticity error and estimate the experimental convergence rate m by using

$$\frac{E(h = 1/32)}{E(h = 1/64)} \approx 2^m.$$

Table I. Boundary condition formula names and their abbreviations

Method	Equations	Abbreviation
Jensen (Briley)	(8)	Jensen
Computational boundary method	(10), (11)	CBM
2nd order compact	(15)	2OC
3rd order compact (Woods)	(19)	3OC
4th order compact	(24)	4OC
4th order compact w/HOC	(26)	4OC/H
4th order compact w/upwind	(27)	4OC/U
High-order Jensen	(29)	HOJ

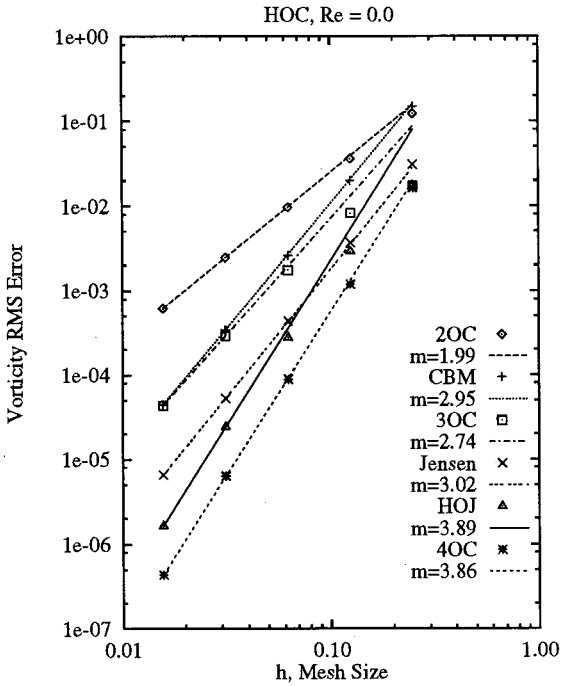

Figure 1. Convergence of vorticity RMS error with respect to mesh size for various boundary condition formulas and $Re = 0$.

Table I is a compilation of the boundary condition abbreviations used throughout this paper. The results for these boundary conditions are plotted in Figure 1.

Clearly, the second-, third-, and fourth-order compact formulas converge at the predicted rates. The Jensen formula converges at the predicted rate of $m = 3$, but is more accurate than the 3OC method. These results verify the interpretation of the truncation error made in Section 2, and illustrate the point that the equation being approximated by these formulas is $\partial\psi/\partial n = \pm V_w$. It is thus reasonable to assume that other formulas, derived in a similar manner and expressed as

$$\zeta(\partial\Omega) = \cdots + O(h^m),$$

are in fact more accurate than reported by a factor of $O(h)$.

Surprisingly, the CBM, for which we would expect to see $O(h^2)$ convergence (because of the use of Equation (11)), actually converges at $m = 3$. This phenomenon is not presently understood, but one theory is that the data presented is not yet asymptotic, and the $O(h^2)$ degradation only appears at smaller mesh sizes. However, the RMS vorticity error for the CBM at $h = 1/128$ is 5.737×10^{-6}, which is still $O(h^3)$.

4. PERFORMANCE STUDIES

If a high-order method takes a significantly longer time to achieve its more accurate results, it may not be worth the extra expense. Conversely, if two methods of roughly equal accuracy converge at different rates, the faster one can be considered superior. Our goal now is to

determine for a given amount of computational 'work,' which boundary condition formula yields the greatest accuracy. This will depend on the solution algorithm used and the definition of work within the context of that algorithm.

The algorithm used here is simple, decoupled, successive approximations, as used by Gupta [8] and Spotz and Carey [10]. This can be viewed as a block-iterative solution of the coupled problem, as described in Reference [10]. This usually requires that the solution procedure to be relaxed in order to prevent divergence. Li *et al.* [9] used a more sophisticated Newton algorithm which was demonstrably more efficient, but the important consideration here is that the same algorithm is used for the different boundary condition formulas for comparison purposes. Gupta *et al.* [22–24], Altas *et al.* [25] and Zhang [26] have experimented with multigrid methods for HOC formulas, which would also be an appropriate solution algorithm.

Conjugate gradient (CG) is used to solve the HOC approximation to Equation (3) and generalized minimum residual (GMRES) is used to solve the non-symmetric HOC approximation to Equation (4), in contrast to Gupta and Li, who both employed point-SOR for both HOC approximations.

Computational 'work' is defined as the total number of cumulative inner iterations (i.e. iterations performed solving the matrix problems, as opposed to the outer, successive approximation iterations). In the context of the successive approximation algorithm, two user-defined quantities affect the amount of work required to converge. First is the relaxation parameter, ω, which if too small can prevent the algorithm from advancing quickly enough in each stage. If too large, it can cause successive overshoots or divergence. The second parameter is the linear iterations limit $\mathscr{L}$ which imposes a maximum on the number of inner iterations that can be performed during each outer iteration. If set too small, then large inaccuracies are allowed to propagate from one outer iteration to the next. If set too large, then iterations are wasted, especially early in the algorithm, trying to converge toward inaccurate intermediate solutions.

Optimal values for ω and $\mathscr{L}$ ostensibly depend on the formula being used, the mesh size, and the Reynolds number Re. Informal experiments were conducted to determine near-optimal combinations of ω and $\mathscr{L}$ for the different boundary condition formulas. To facilitate these experiments, a relatively coarse mesh of $h = 1/16$ was used. The final combinations are shown in Table II.

Interestingly, these combinations were the same for $Re = 0$ and 100 for any given method, implying that Re does not, in fact, have a significant effect on the optimal values of ω and $\mathscr{L}$.

Figures 2 and 3 show the accuracy of the various methods as a function of cumulative inner iterations, for $Re = 0$ and 100 respectively. Most of the methods (with the exception of CBM) converge at roughly the same rate. Thus for these methods, the high-order formulas are as efficient as the low-order formulas. The CBM however, converges at a slightly faster rate than the other methods, making it vastly superior to the 2OC method (which converges more slowly

Table II. Near-optimal values of the relaxation parameter ω and the inner iteration limit $\mathscr{L}$ for various boundary condition formulas at $h = 1/16$

Method	ω	$\mathscr{L}$
Jensen	0.55	8
CBM	0.93	8
2OC	0.65	8
3OC	0.60	10
4OC	0.60	10
HOJ	0.55	10

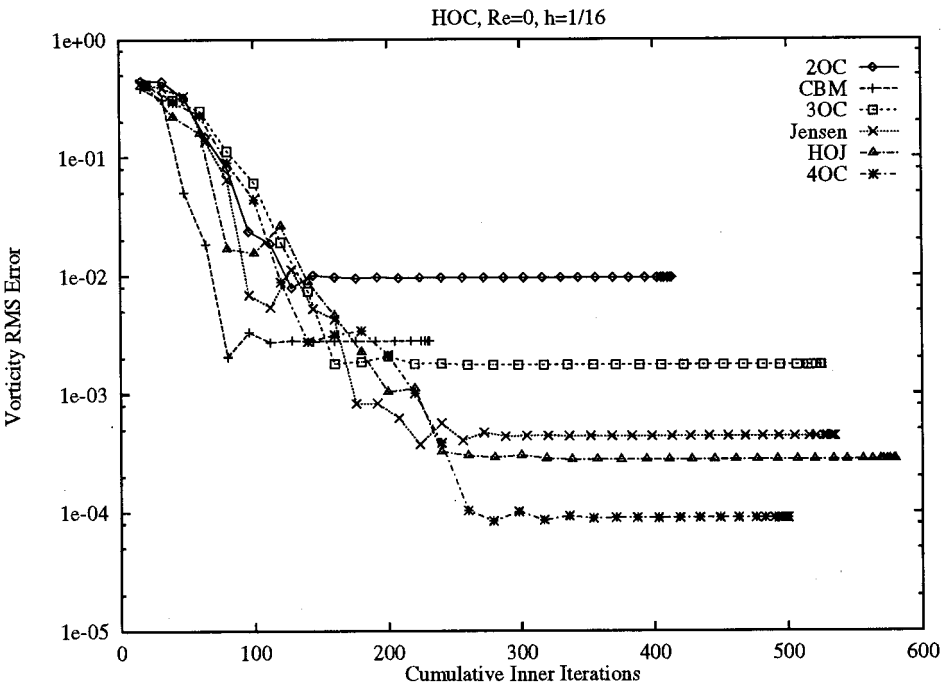

Figure 2. Convergence of vorticity RMS error with respect to iterations for various boundary condition formulas at $h = 1/16$ and $Re = 0$.

to a less accurate solution), and superior to the 3OC method (which converges more slowly to roughly the same accuracy).

The faster convergence of the CBM is probably due to the higher permissible value of ω. However, the accuracy of the CBM is not as good as the accuracy of Jensen, HOJ or the 4OC method. This may suggest the utility of a hybrid method which switches from CBM to a more accurate method once the CBM has converged.

5. DRIVEN CAVITY STUDIES

We turn our attention now to using the various boundary condition formulas to solve the standard benchmark problem of a lid-driven square cavity of fluid. The case $Re = 1000$ is chosen, for which there is general agreement that the HOC method can produce a reasonably accurate solution on a 41×41 grid [8–10]. For comparison purposes, we can refer to the uniform grid solutions of Ghia, Ghia and Shin [27], who solved the $Re = 1000$ case on a 129×129 grid.

The differences between the analytic model problem and the driven cavity problem (non-zero forcing function versus $f = 0$ and stationary walls versus one moving wall) are enough to drastically change the convergence properties exhibited by the various boundary condition formulas. Surprisingly, the CBM, which showed the best convergence properties for the model problem, was the most sensitive to user choices such as starting guess, relaxation parameter, inner iteration limit, and continuation steps. It took by far the longest to converge, yet it resulted in the best approximation by various measures. Certain formulas, such as the 4OC

schemes with corrections, were especially sensitive to the initial guess, converging to a better answer given a better initial guess.

In order to compare performance in a sense that could be considered 'fair,' all the methods were run with the same algorithm parameters. This was overkill for some methods (e.g. 2OC and 3OC could converge from the initial guess of zero without continuation), but necessary for others to converge. The algorithm was started with an initial guess generated by 2OC BCs at $Re = 500$, and was stepped to $Re = 500$ (to generate the differences incurred by the BC formulas), $Re = 600$, 700, 800, 900 and finally 1000. A relaxation parameter $\omega = 0.6$ and inner iteration limit $\mathscr{L} = 10$ was used. Letting

$$E(n) = \frac{\sum_{i,j} |\zeta_{ij}^n - \zeta_{ij}^{n-1}|}{\sum_{ij} \zeta_{ij}^n} + \frac{\sum_{i,j} |\psi_{ij}^n - \psi_{ij}^{n-1}|}{\sum_{ij} \psi_{ij}^n},$$

the algorithm was terminated when $E(n) < 10^{-6}$.

Surprisingly, the quickest convergence was achieved by the corrected 4OC schemes, with the upwind correction converging in only 135 iterations, and the HOC correction converging in 430 iterations. But as we will see, these solutions were the two least satisfactory. The rest of the methods ranked as follows: 2OC (925 iterations), HOJ (1280), 3OC (1301), Jensen (1331), and 4OC (2231). The CBM failed to converge within 6000 iterations, although it should be noted that Li *et al.* had success with the CBM using a Newton algorithm.

Figures 4–11 show the streamfunction and vorticity contours (using the contour values standardized by Ghia) for HOC solutions using 2OC, 3OC, 4OC, 4OC/H, 4OC/U, CBM,

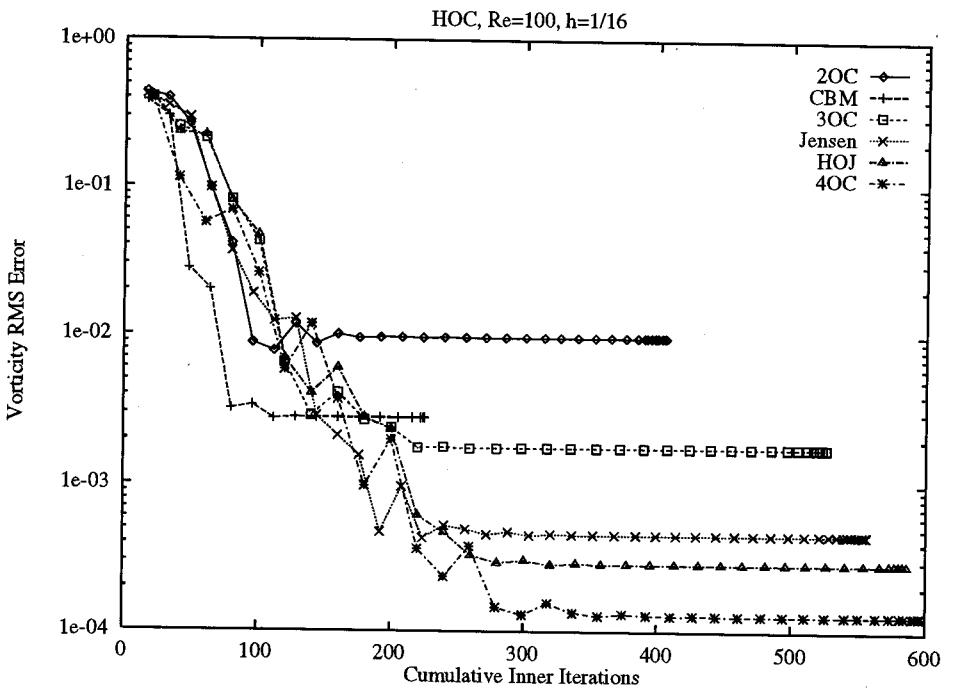

Figure 3. Convergence of vorticity RMS error with respect to iterations for various boundary condition formulas at $h = 1/16$ and $Re = 100$.

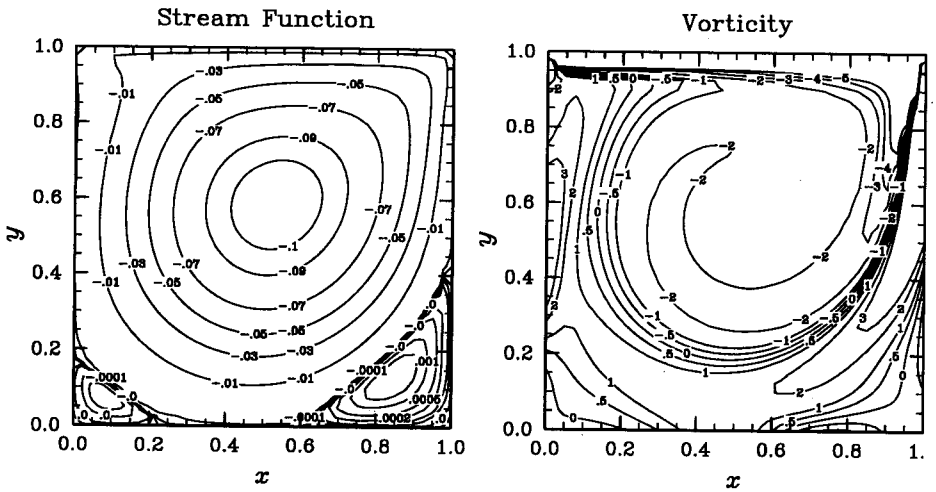

Figure 4. Second-order compact (2OC) boundary conditions for the lid-driven cavity problem, $Re = 1000$ on a 41×41 grid.

Jensen, and HOJ boundary condition formulas, respectively. Qualitatively, these plots are very similar, but with subtle differences. Note, for example, the minimum streamfunction contours for the primary vortex, and the -2 'finger' in the vorticity plots. Only the 3OC, CBM, Jensen, and HOJ methods capture this finger extending as far as Ghia predicts.

Clearly, the 4OC/H results in Figure 7 are the most disappointing. The correction term intended to suppress the oscillations in the vorticity for the 4OC formulation (not even evident in Figure 6 due to the chosen contour levels) does more harm than good. This may be due to the fact that the truncation error for Equation (27), while $O(h^4)$, is also proportional to Re^2, which imposes too large an error at this mesh size.

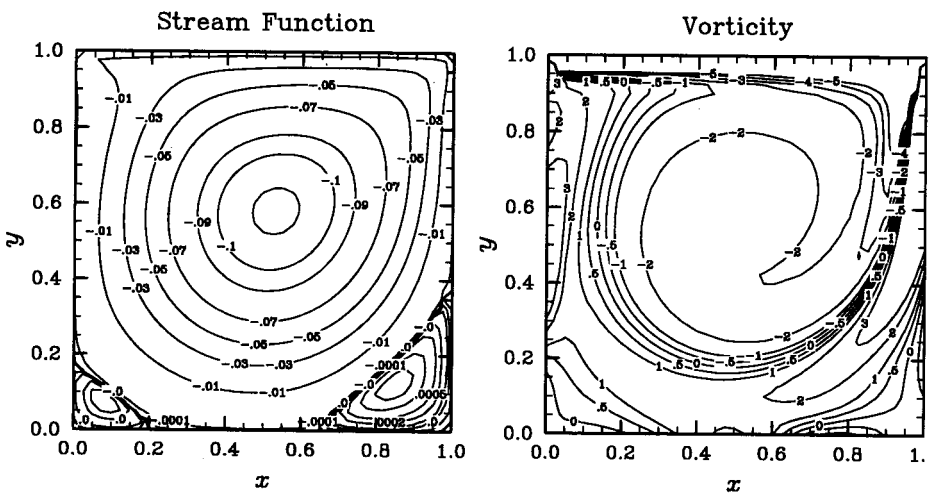

Figure 5. Third-order compact (3OC) boundary conditions for the lid-driven cavity problem, $Re = 1000$ on a 41×41 grid.

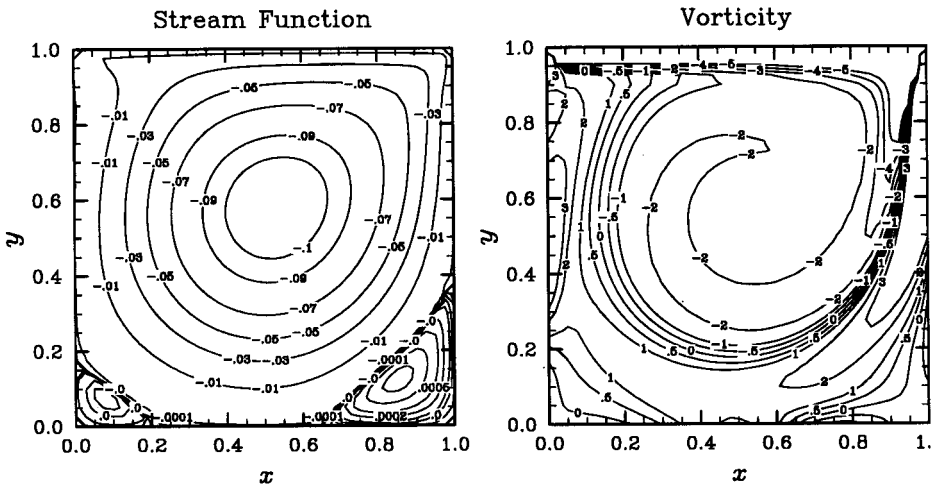

Figure 6. Fourth-order compact (4OC) boundary conditions for the lid-driven cavity, $Re = 1000$ on a 41×41 grid.

Figure 12 plots the vorticity on the moving lid for the various boundary conditions (with the exception of the CBM, which does not solve for ζ on the boundary). None of the methods capture the vorticity near the corner singularities very well, which is to be expected, since all of the formulas assume greater smoothness than is found in the neighborhood of the corners. The 3OC, Jensen, and HOJ formulas give very good agreement, but the inaccuracy of the 2OC method is evident. All three of the 4OC plots demonstrate unacceptably high error. Apparently, using the vorticity transport equation (4) as a high-order substitution introduces dominating truncation error terms when Re is sufficiently high.

The same conclusions can be drawn regarding the plots of the horizontal velocity component along the cavity centerline, shown in Figure 13. 2OC, 3OC, Jensen and HOJ produce similarly acceptable results, while the 4OC formulas are generally good, but somewhat in error near the bottom wall. The CBM results are very good for this case.

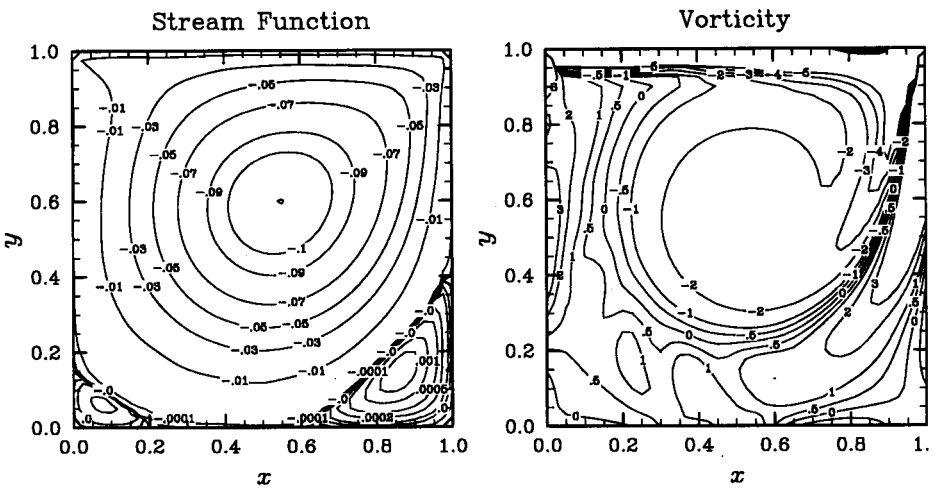

Figure 7. Fourth-order compact boundary conditions with high-order correction (4OC/H) for the lid-driven cavity problem, $Re = 1000$ on a 41×41 grid.

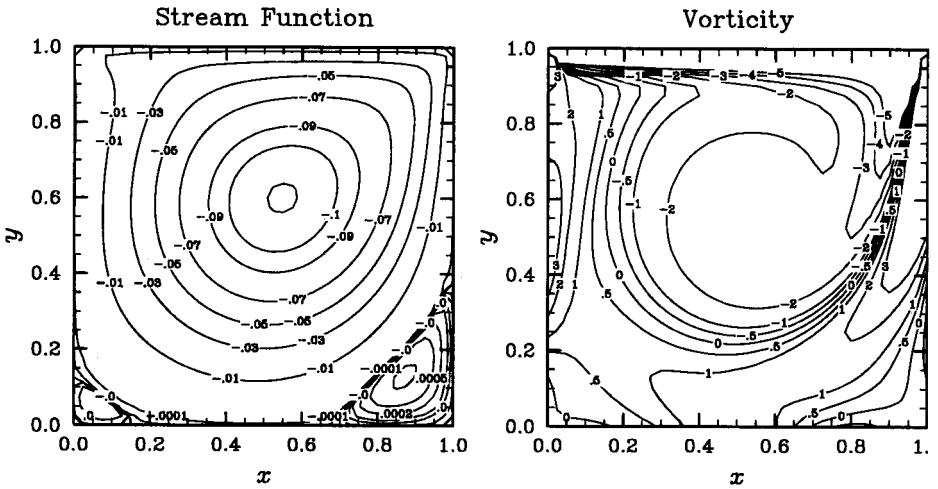

Figure 8. Fourth-order compact boundary conditions with upwind correction (4OC/U) for the lid-driven cavity problem, $Re = 1000$ on a 41×41 grid.

We now look at the strength, location, and size of the three vortices (primary, bottom left and bottom right) present in this problem to the results of Ghia (a second bottom right vortex is known to exist, but cannot be resolved with the present grid). This should give us some indication of the relative ability of the different methods to capture the overall flow pattern.

Table III reports the values of ψ, ζ and the location of the primary vortex. CBM captures the transport variables best. Table IV shows the same data, plus the horizontal length H and the vertical length V of the bottom left corner vortex. Again, CBM produces the best ψ and ζ, but Jensen predicts the best H and HOJ the best V. Finally, Table V repeats the same data for the bottom right vortex. Interestingly, despite their failure to accurately capture the vorticity behavior on the moving lid, 4OC predicts the best ψ and 4OC/U predicts the best H and V. CBM captures ζ best in the bottom right corner.

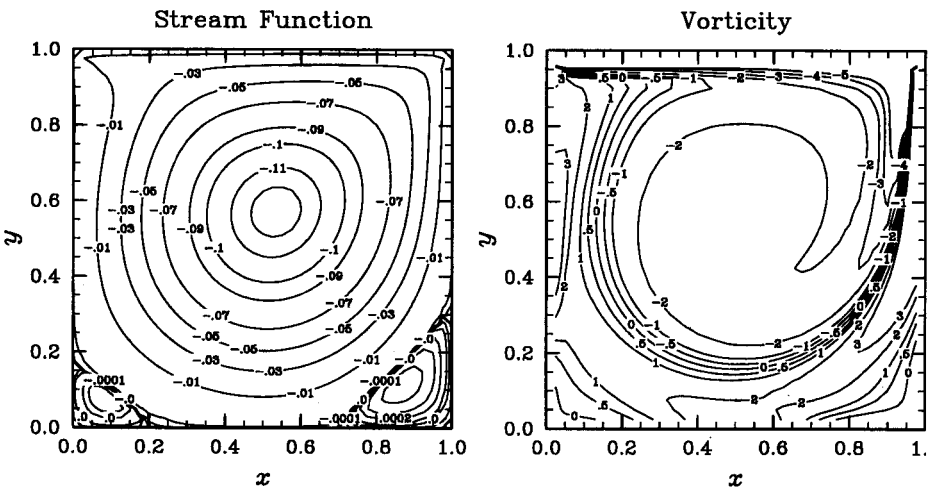

Figure 9. Computational boundary method (CBM) for the lid-driven cavity problem, $Re = 1000$ on a 41×41 grid.

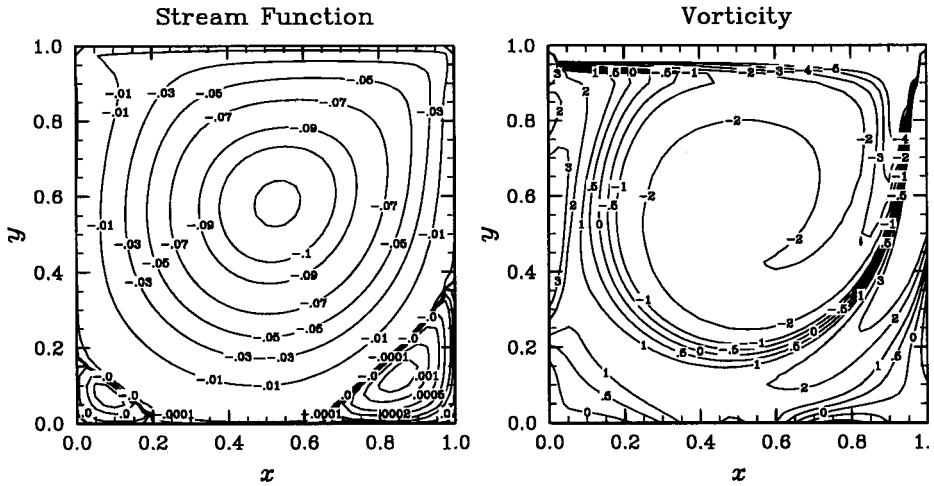

Figure 10. Jensen boundary conditions for the lid-driven cavity problem, $Re = 1000$ on a 41×41 grid.

6. SUMMARY

Since at least 1928, there has been interest in methods to handle no-slip boundary conditions for the (ψ, ζ) system. The earliest attempts using Taylor series resulted in a formula which predicted $O(h)$ accuracy at the boundaries, but recent studies in the context of a fourth-order compact interior discretization have shown it to be $O(h^2)$. This has led to a re-evaluation of the truncation error analysis of the standard Taylor series approach, which in turn has led to the observation here that other well-known formulations, such as Jensen's and Woods' (here referred to as third-order compact), are $O(h^3)$, not $O(h^2)$.

The fourth-order compact interior scheme has also motivated a search for boundary conditions which are also high-order and compact. This paper has examined the formulas

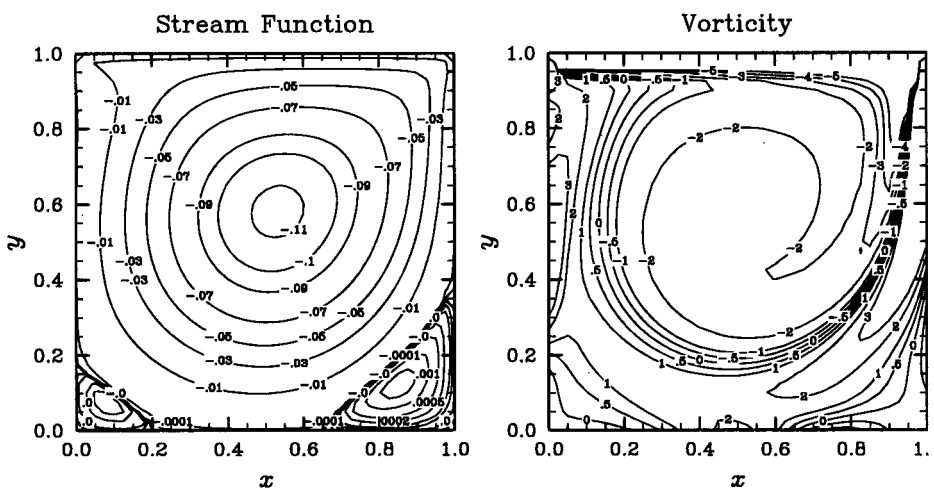

Figure 11. High-order Jensen (HOJ) boundary conditions for the lid-driven cavity problem, $Re = 1000$ on 41×41 grid.

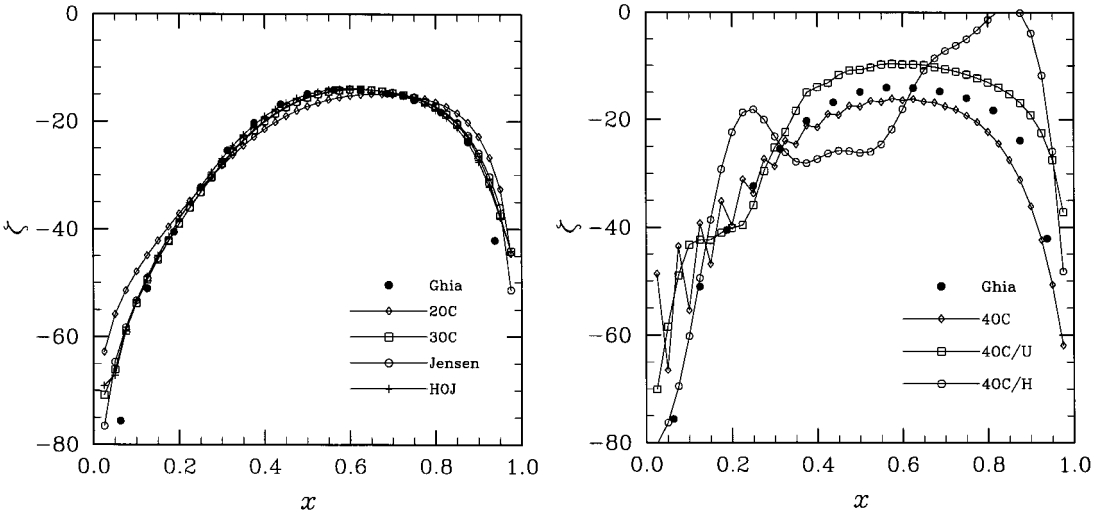

Figure 12. Vorticity on the moving lid of a driven cavity, $Re = 1000$, for various boundary conditions on a 41×41 grid, compared with the results of Ghia, on a 129×129 grid.

already mentioned, the computational boundary method, and the fourth-order compact formulation. In addition, three new formulas were proposed, including two corrections to the 4OC formula, and a fourth-order version of the Jensen formula.

The different formulations were tested first using an analytic model problem. This allowed experimental verification of the predicted solution error rates and comparison of the convergence properties. They were tested next on the driven cavity problem, comparing streamfunction and vorticity contours, wall vorticity plots, cross-sectional velocity plots, and vortex data with published results on a much finer mesh. Driven cavity convergence results shed doubt on the utility of using the model problem convergence properties in any predictive way.

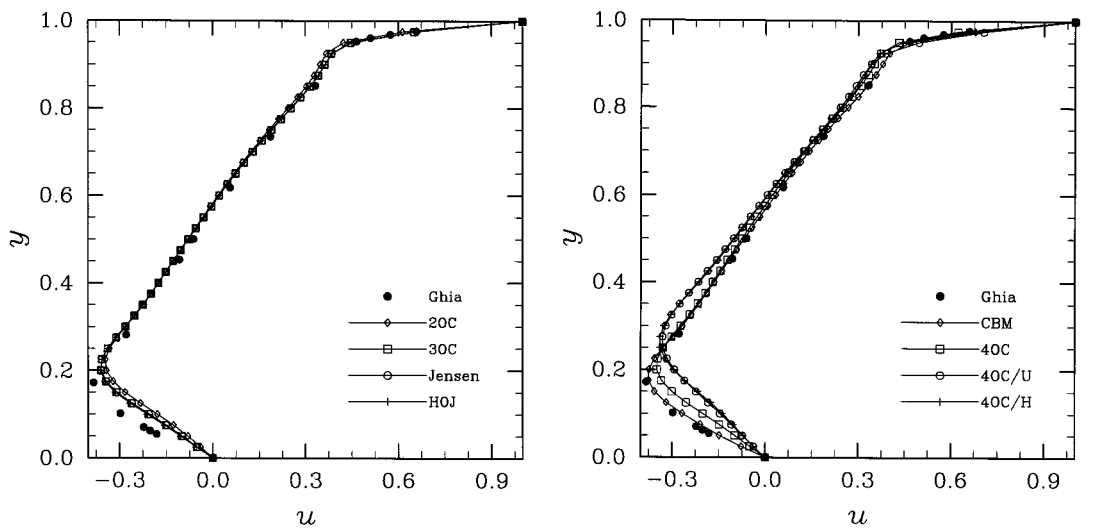

Figure 13. Horizontal velocity along the vertical centerline of a driven cavity, $Re = 1000$, for various boundary conditions on a 41×41 grid, compared with the results of Ghia, on a 129×129 grid.

Table III. Primary vortex data for the lid-driven cavity problem, $Re = 1000$ on a 41×41 grid, for various boundary condition formulas

Method	ψ	ζ	(x, y)
Ghia	−0.117929	−2.04968	0.5313, 0.5625
2OC	−0.106967	−1.97142	0.5250, 0.5750
3OC	−0.111965	−2.03173	0.5250, 0.5750
4OC	−0.108915	−1.98109	0.5250, 0.5750
4OC/H	−0.110088	−2.18602	0.5500, 0.6000
4OC/U	−0.110898	−2.18352	0.5500, 0.6000
CBM	**−0.117240**	**−2.05332**	0.5250, 0.5750
Jensen	−0.111907	−2.03300	0.5250, 0.5750
HOJ	−0.112435	−2.03313	0.5250, 0.5750

The best approximations are in bold face.

Table IV. Bottom left vortex data for the lid-driven cavity problem, $Re = 1000$ on a 41×41 grid, for various boundary condition formulas

Method	ψ	ζ	(x, y)	H	V
Ghia	0.000231	0.36175	0.0859, 0.0781	0.2188	0.1680
2OC	0.000160	0.19629	0.0750, 0.0750	0.2120	0.1595
3OC	0.000148	0.20976	0.0750, 0.0750	0.2194	0.1640
4OC	0.000138	0.20486	0.0750, 0.0750	0.2173	0.1627
4OC/H	0.000066	0.17261	0.0750, 0.0750	0.2240	0.1431
4OC/U	0.000036	0.10595	0.0750, 0.0500	0.1729	0.1303
CBM	**0.000174**	**0.23915**	0.0750, 0.0750	0.1281	0.1093
Jensen	0.000150	0.20968	0.0750, 0.0750	**0.2189**	0.1631
HOJ	0.000150	0.21298	0.0750, 0.0750	0.2193	**0.1641**

The best approximations are in bold face.

The accuracy and performance of the various formulas for the driven cavity problem are now summarized. The 2OC (or standard Taylor series) formula had good convergence but only fair accuracy. The 3OC (or Woods) formula also had good convergence, as well as good accuracy. 4OC converged poorly but had fair accuracy, except on the moving lid, where oscillations appear. 4OC is best suited for stationary walls only. The corrected 4OC schemes,

Table V. Bottom right vortex data for the lid-driven cavity problem, $Re = 1000$ on a 41×41 grid, for various boundary condition formulas

Method	ψ	ζ	(x, y)	H	V
Ghia	0.001751	1.15465	0.8594, 0.1094	0.3034	0.3536
2OC	0.002057	0.87004	0.8500, 0.1250	0.3672	0.3992
3OC	0.001818	1.00094	0.8500, 0.1250	0.3470	0.3956
4OC	**0.001731**	0.98470	0.8500, 0.1250	0.3425	0.3925
4OC/H	0.001846	0.94158	0.8500, 0.1500	0.3756	0.4339
4OC/U	0.001114	0.55195	0.8750, 0.1250	**0.3067**	**0.3856**
CBM	0.001360	**1.04409**	0.8750, 0.1250	0.2330	0.2329
Jensen	0.001842	0.99143	0.8500, 0.1250	0.3490	0.3970
HOJ	0.001781	1.02872	0.8500, 0.1250	0.3424	0.3900

The best approximations are in bold face.

4OC/H and 4OC/U, both converged very quickly to inaccurate solutions. The results were particularly bad on the moving lid, where the corrections were intended to suppress oscillations seen in the 4OC method. Instead, they introduced unacceptable truncation errors proportional to Re (4OC/U) and Re^2 (4OC/H).

The CBM was perhaps the most surprising formula tested. Experimental error rates are $O(h^3)$, despite the use of standard second-order central differencing near the border. CBM converged well for the analytic model problem, but extremely poorly for the driven cavity. Nevertheless, CBM results were among the best observed, based upon the contour plots, velocity plot, and vortex data. The drawback of the CBM is that ζ is not computed on the boundary, but this could be corrected in a post-processing step using one of the other formulas.

Both the Jensen and high-order Jensen formulas had fair convergence and good accuracy, with HOJ giving slightly better approximations in most cases. As such, the HOJ formula marginally gives the best combination of accuracy and performance of all the formulas studied. Both methods are non-compact, since they use data a distance $2h$ from the boundary. However, this is still a small stencil and its use does not violate any of the primary advantages of compact stencils: that compact stencils require less communication when the scheme is parallelized via domain decomposition, and eliminating the need for special formulas near the boundaries.

Given the disparity of convergence results (4OC/U converged to a driven cavity solution for $Re = 1000$ in 135 iterations while CBM failed to meet the same converge criteria in 6000 iterations), it is clear that the boundary condition formulas control the convergence of the successive approximation algorithm used here. This is because for most of the formulas (except CBM), the vorticity on the wall represents a high-order correction to an approximation to $\boldsymbol{V}_w = \pm \partial\psi/\partial n$. This does not allow the wall vorticity to influence the successive approximations efficiently.

Although the boundary conditions have been studied here in the context of steady state problems, most of them could be applied to transient problems. Only the 4OC formula and its 'corrections' are not currently usable in a time-dependent problem. This is because they utilize the vorticity transport equation to model high-order truncation terms, and this equation is slightly different in a transient setting. The term $\partial\zeta/\partial t$ would have to be accounted for.

ACKNOWLEDGMENTS

The author is supported by the Advanced Studies Program at the National Center for Atmospheric Research and would like to thank Paul Swarztrauber, Bob Kerr, Steve Hammond, Beth Wingate and the reviewers for their comments and suggestions. NCAR is sponsored by the National Science Foundation.

REFERENCES

1. M.M. Gupta, R.P. Manohar and J.W. Stephenson, 'A single cell high order scheme for the convection–diffusion equation with variable coefficients', *Int. J. Numer. Methods Fluids*, **4**, 641–651 (1984).
2. M.M. Gupta, R.P. Manohar and J.W. Stephenson, 'High-order difference schemes for two-dimensional elliptic equations. *Numer. Methods Partial Differ. Equ.*, **1**, 71–80 (1985).
3. S.C.R. Dennis and Q. Wing, 'Generalized finite differences for operators of Navier–Stokes type', in F.G. Zhuang and Y.L. Zhu (eds.), *Proc. 10th International Conference on Numerical Methods in Fluid Dynamics*, Vol. 264 of Lecture Notes in Physics, Springer-Verlag, Berlin, 1986, pp. 222–228.
4. R.J. MacKinnon and G.F. Carey, 'Analysis of material interface discontinuities and superconvergent fluxes in finite difference theory', *J. Comput. Phys.*, **75**, 151–167 (1988).

5. S.C.R. Dennis and J.D. Hudson, 'Compact h^4 finite difference approximations to operators of Navier–Stokes type', *J. Comput. Phys.*, **85**, 390–416 (1989).
6. R.J. MacKinnon and R.W. Johnson, 'Differential equation based representation of truncation errors for accurate numerical simulation', *Int. J. Numer. Methods Fluids*, **13**, 739–757 (1991).
7. W.F. Spotz, 'High-order compact finite difference schemes for computational mechanics', *Ph.D. Thesis*, University of Texas at Austin, December 1995.
8. M.M. Gupta, 'High accuracy solutions of incompressible Navier–Stokes equations', *J. Comput. Phys.*, **93**, 343–359 (1991).
9. M. Li, T. Tang and B. Fornberg, 'A compact fourth-order finite difference scheme for the steady incompressible Navier–Stokes equations', *Int. J. Numer. Methods Fluids*, **20**, 1137–1151 (1995).
10. W.F. Spotz and G.F. Carey, 'High-order compact scheme for the stream-function vorticity equations', *Int. J. Numer. Methods Eng.*, **38**, 3497–3512, (1995).
11. S.A. Orszag and M. Israeli, 'Numerical simulation of viscous incompressible flows', *Annu. Rev. Fluid Mech.*, **6**, 281–318 (1974).
12. M.M. Gupta and R.P. Manohar, 'Boundary approximations and accuracy in viscous flow computations', *J. Comput. Phys.*, **31**, 265–288 (1979).
13. P.M. Gresho, 'Incompressible fluid dynamics: Some fundamental formulation issues', *Annu. Rev. Fluid Mech.*, **23**, 413–453 (1991).
14. T.Y. Hou and B.T.R. Wetton, 'Convergence of a finite difference scheme for the Navier–Stokes equations using vorticity boundary conditions', *SIAM J. Numer. Anal.*, **29**, 615–639 (1992).
15. P. Roache, *Computational Fluid Dynamics*, Hermosa Press, Albuquerque, NM, 1972.
16. V.G. Jensen, 'Viscous flow round a sphere at low Reynolds number (≤ 40)', *Proc. Roy. Soc. Lond., Series A*, **249**, 346–366 (1959).
17. C.E. Pearson, 'A computational method for viscous flow problems', *J. Fluid Mech.*, **21**, 611–622 (1965).
18. W.R. Briley, 'A numerical study of laminar separation bubbles using the Navier–Stokes equations', *Technical Report J110614-1*, United Aircraft Research Laboratories, East Hartford, Connecticut, 1970.
19. H. Huang and H. Yang, 'The computational boundary method for solving the Navier–Stokes equations', *Technical Report 90-5*, The Institute of Applied Mathematics and Statistics, The University of British Columbia, Vancouver, Canada, July 1990.
20. A. Thom, 'An investigation of fluid flow in two dimensions', *Technical Report 1194*, Aerospace Research Center, United Kingdom, 1928.
21. L.C. Woods, 'A note on the numerical solution of fourth order differential equations', *Aeronaut. Q.*, **5**, 176 (1954).
22. M.M. Gupta, J. Kouatchou and J. Zhang, 'A compact multigrid solver for convection–diffusion equations', *J. Comput. Phys.*, to appear.
23. M.M. Gupta, J. Kouatchou and J. Zhang, 'Comparison of second- and fourth-order discretizations for multigrid Poisson solvers', *J. Comput. Phys.*, **132**, 226–232 (1997).
24. M.M. Gupta, J. Kouatchou and J. Zhang, 'Preconditioning free multigrid method for convection–diffusion equations with variable coefficients', unpublished, 1995.
25. I. Altas, J. Dym, M.M. Gupta and R.P. Manohar, 'Multigrid solution of automatically generated high order discretizations for the biharmonic equation', *SIAM J. Sci. Comput.*, to appear.
26. J. Zhang, 'Accelerated multigrid high accuracy solution of the convection–diffusion equation with high Reynolds number', *Numer. Methods Partial Differ. Equ.*, **13**, 77–92 (1997).
27. U. Ghia, K.N. Ghia and C.T. Shin, 'High *Re* solutions for incompressible flow using Navier–Stokes equations and a multi-grid method', *J. Comput. Phys.*, **48**, 387–411 (1982).

